



## Pulsed electron–electron double resonance (PELDOR) distance measurements in detergent micelles

Bela E. Bode<sup>1</sup>, Reza Dastvan, Thomas F. Prisner<sup>\*</sup>

*Institute of Physical and Theoretical Chemistry and Center for Biomolecular Magnetic Resonance, Goethe University, Max-von-Laue-Strasse 7, 60438 Frankfurt am Main, Germany*

### ARTICLE INFO

#### Article history:

Received 21 December 2010

Revised 9 March 2011

Available online 17 March 2011

#### Keywords:

Pulsed electron paramagnetic resonance (EPR)

Double electron–electron resonance (DEER)

Pulsed dipolar spectroscopy

Detergent solubilization

Membrane protein

### ABSTRACT

Pulsed electron–electron double resonance (PELDOR) spectroscopy is a powerful tool for measuring nanometer distances in spin-labeled systems. A common approach is doubly covalent spin-labeling of a macromolecule and measurement of the inter-spin distance, or to use singly-labeled components of a system that forms aggregates or oligomers. This situation has been described as a spin-cluster. The PELDOR signal, however, does not only contain the desired dipolar coupling between the spin-labels of the molecule or cluster under study. In samples of finite concentration the dipolar coupling between the spin-labels of the randomly distributed molecules or spin-clusters also contributes significantly. In homogeneous frozen solutions or lipid vesicle membranes this second contribution can be considered to be an exponential or stretched exponential decay, respectively. In this study, we show that this assumption is not valid in detergent micelles. Spin-labeled fatty acids that are randomly partitioned into different detergent micelles give rise to PELDOR time traces which clearly deviate from stretched exponential decays. The obtained signals can be modeled quantitatively based on the size of the micelles, their aggregation number, the spin-label concentration and the degree of spin-labeling. As a main conclusion a PELDOR signal deviating from a stretched exponential decay does not necessarily prove the observation of specific distance information on the molecule or cluster. These results are important for the interpretation of PELDOR experiments on membrane proteins or lipophilic peptides solubilized in detergent micelles or small vesicles, which often do not show pronounced dipolar oscillations in their time traces.

© 2011 Elsevier Inc. All rights reserved.

### 1. Introduction

Pulse EPR distance measurements have evolved to a standard tool for generating long-range constraints for structural modeling. Especially the pulsed electron–electron double resonance (PELDOR) [1,2] method has found widespread application in many fields [3,4]. One approach is to covalently attach two spin-labels to a macromolecule and measure the inter-spin distance. Alternatively, singly-labeled components of a system that forms aggregates or oligomers can be employed. This situation has been referred to as a spin-cluster. The inter-spin distance is calculated from the dipolar coupling between the spin-labels in such a spin-cluster, giving access to information on the oligomerization state and structure of the cluster. The PELDOR signal, however, does not only contain these desired dipolar couplings. In samples of finite concentration the dipolar coupling between the randomly distributed spin-clusters also contributes significantly. All methods to derive structural information from PELDOR time traces rely on

the assumption that the inter-cluster background signal can be separated from the specific intra-cluster interaction under study. However, an erroneous assumption of the background function can cause artifacts in the data analysis. In frozen solutions of model compounds in organic solvents [5–7], soluble proteins [8,9], or nucleic acids [10,11] the distribution of spin-clusters can be approximated to be homogeneous in three-dimensional space. The background signal corresponding to such a distribution is an exponential decay function [12]. The distribution of spin-clusters in lipid vesicle membranes can also be assumed to be homogeneous. The dimension of this homogeneous distribution varies from two to three depending on the sample concentration [13–15]. This corresponds to a stretched exponential decay function describing the background [16]. In contrast to homogeneous solutions and lipid vesicles, spin-labels in detergent micelles are confined to small volumes. This leads to an inhomogeneous distribution of spin-clusters on the length scale accessible by the PELDOR method. Several earlier works have relied on PELDOR to investigate size restriction effects in microscopic assemblies. Ruthstein *et al.* have characterized micelles with respect to micelle size and aggregation number. The micelles were formed from pluronic block copolymers built from chains of poly(ethylene oxide) and poly(propylene oxide) [17]. In a second study the formation

<sup>\*</sup> Corresponding author. Fax: +49 69 798 29404.

E-mail address: [prisner@chemie.uni-frankfurt.de](mailto:prisner@chemie.uni-frankfurt.de) (T.F. Prisner).

<sup>1</sup> Present address: Leiden Institute of Chemistry, Leiden University, Einsteinweg 55, 2333 CC Leiden, The Netherlands.

of mesoporous materials from solutions of these micelles was monitored using PELDOR [18]. Mao et al. investigated the local structures in organically modified layered silicates and their composites with polymers. PELDOR on spin-labeled surfactants allowed the extraction of local spin concentrations and the fractal dimension of the homogeneous spin distribution [19]. The lateral diffusion of spin-labeled thiols on spherical gold nanoparticles has been studied by Ionita et al. The spin–spin distance distribution function was extracted from PELDOR data [20].

In this study, we investigated the effects of these size restriction on the PELDOR signal especially on micelles formed from detergents that are frequently used for solubilization of membrane proteins [21]. Therefore, we explored the characteristics of the intermolecular dipolar interactions between single spin-labeled fatty acid molecules statistically partitioned into detergent micelles. We have chosen spin-labeled fatty acids instead of large macromolecules as test system, because they do not give rise to large exclusion volumes, the conformational freedom of the spin-label moiety is less hindered and the structure of the micelle will be less distorted.

We find that the resulting time traces cannot be described by stretched exponential decay functions but can be simulated based on literature values for the detergent micelles dimensions and aggregation numbers and a statistic distribution of spin-labels inside the micelles. Since a specific interaction between the spin-probes is not observed, these statistic aggregates resemble a background function for detergent micelles. Understanding the background signal in detergent micelles is of importance for spin-labeled membrane proteins and peptides solubilized in detergent micelles or small vesicles for PELDOR measurements.

## 2. Modeling of time traces

Owing to their amphipathic nature, spin-labeled fatty acids are expected to be confined inside the micelles. To model the observed PELDOR decays we used two limiting models for the description of the distribution of spin-labels inside the micelles. In both models the micelles are assumed to be spherical. In the first model the nitroxyl groups of the spin-labels are assumed to be close to the surface of the micelle (*surface* model). This might be induced by either steric repulsion inside the micelle or by strong attraction between the polar nitroxide moiety and the polar detergent head-groups [22]. The other limiting model assumes a homogeneous distribution of the nitroxides inside the micelle (*bulk* model). These simplified models are chosen because analytical expressions for the statistical distance distribution functions are easily available for both models. The probability density distribution for the distance between two points on the surface of a sphere is [23]:

$$P_{surf}(r) = \frac{2r}{D^2} \quad (1)$$

where  $r$  is the distance between the points and  $D$  the diameter of the sphere.

The probability density distribution for the distance between two points inside a sphere is [24]:

$$P_{bulk}(r) = \frac{3r^2}{(D/2)^3} - \frac{9r^3}{4(D/2)^4} + \frac{3r^5}{16(D/2)^6} \quad (2)$$

The real situation is most probably best reflected by the spin-labeled fatty acids occupying a sphere shell with a certain width. In this case, the two models represent two limiting approximations of the actual distribution which will depend on the specific spin-label [25]. Both limiting models allow simulating the experimentally observed non-exponential PELDOR decay curves; therefore the actual distribution function is dispensable for our analysis.

The probability of finding a micelle with  $k$  spin-labeled fatty acid molecules is estimated by the binomial distribution:

$$P_{label}(k) = \binom{n}{k} p^k (1-p)^{n-k} \quad (3)$$

with  $n$  being the number of detergent molecules per micelle (aggregation number) and  $p$  the probability of a detergent being spin-labeled (labeling degree). The binomial coefficients for the case  $n = 100$  and  $p = 0.01$  are depicted as a histogram in Fig. 1.

The distance dependent dipolar coupling between the spin-labels is calculated according to Eq. (4).

$$v(r, x) = dip(r)(1 - 3x^2) \quad (4)$$

$$dip(r) = \frac{g_A g_B \mu_0 \mu_B^2}{4\pi\hbar} \frac{1}{r^3}$$

where  $v(r, x)$  describes the coupling frequency in dependence of the inverse cube of the spin–spin distance  $r$  and the cosine of the dipolar angle  $\theta$  ( $x = \cos \theta$ ).  $\mu_0$  is the vacuum permeability,  $g_{A,B}$  are the effective values of the  $g$ -tensors of the spins,  $\mu_B$  is the Bohr magneton, and  $\hbar$  is the Planck constant divided by  $2\pi$ .

In both models short spin–spin distances are present. This will give rise to large dipolar couplings, which exceed the excitation bandwidths of the microwave pulses. A correction for the suppression of these large spin–spin interactions can be estimated according to:

$$\lambda(r) = \lambda_0 \int_0^1 \exp\left(-\left(\frac{v(r, x)t_{p1}}{\pi}\right)^2\right) \exp\left(-\left(\frac{v(r, x)t_{p2}}{\pi}\right)^2\right) dx \quad (5)$$

where the integral describes the dipolar frequency ( $v$ )-dependent suppression of intensities as a function of the lengths of the pumping and detection pulses,  $t_{p1}$  and  $t_{p2}$  respectively [26,27].  $\lambda_0$  is the modulation depth parameter which is given by the fraction of the spin-label spectrum excited by the pump pulse. Eq. (5) is a good approximation to rescale the modulation depth for strong dipolar couplings, which effectively diminishes contributions to the PELDOR signal arising from spin pairs with very short distances.

Assuming the orientations of the two spin-labels to be uncorrelated, the PELDOR time trace for a doubly-labeled micelle can be calculated according to [16,28]:

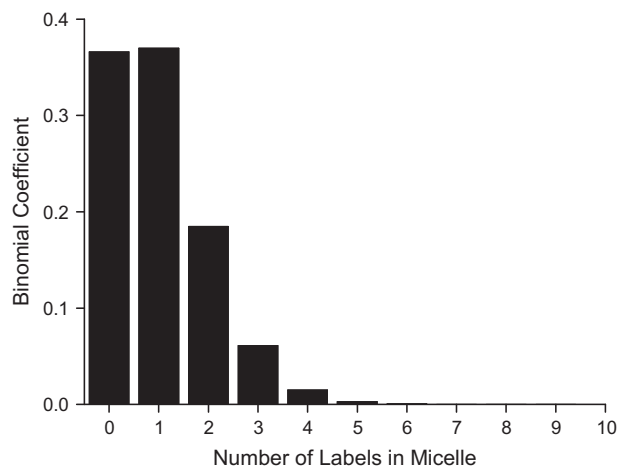


Fig. 1. Binomial coefficients for statistic labeling. The data displayed corresponds to the case of  $n = 100$  and  $p = 0.01$ .

$$\begin{aligned}
 V_{surf}^{pair}(t, D, \lambda_0) &= \int_0^r P_{surf}(r)(1 - \lambda(r)) \int_0^1 (1 - \cos(2\pi v(r, x)t)) dx dr \\
 V_{bulk}^{pair}(t, D, \lambda_0) &= \int_0^r P_{bulk}(r)(1 - \lambda(r)) \int_0^1 (1 - \cos(2\pi v(r, x)t)) dx dr
 \end{aligned}
 \quad (6)$$

where  $t$  is the time delay of the second frequency pulse with respect to the primary Hahn-echo created by the first frequency pulses. It is obvious from Eq. (6) that both the distance distribution function  $P(r)$  and micelle radius  $r$  directly influence the PELDOR signal. The overall signal of the statistically labeled micelle is the weighted sum of the 1-fold to  $n$ -fold labeled micelle [2,29,30]:

$$\begin{aligned}
 V_{surf}(t, D, \lambda_0, p, n) &= \frac{\sum_{k=1}^n P_{label}(k)(V_{surf}^{pair}(t))^{k-1}}{\sum_{k=1}^n P_{label}(k)} \\
 V_{bulk}(t, D, \lambda_0, p, n) &= \frac{\sum_{k=1}^n P_{label}(k)(V_{bulk}^{pair}(t))^{k-1}}{\sum_{k=1}^n P_{label}(k)}
 \end{aligned}
 \quad (7)$$

The normalization is necessary since there is a possibility of zero labels in a micelle ( $k = 0$ ), which does not contribute to the PELDOR signal.

Until here, we have considered only the dipolar interactions between spin-labels in one micelle, however; also interactions between spin-labels in different micelles might contribute to the PELDOR signal. This additional contribution is assumed to be caused by a homogeneous distribution of micelles in three dimensions. For dilute two- to fourfold labeled model compounds an exponential background function has shown excellent agreement with the experimental data [29]:

$$\begin{aligned}
 V_{total}(t, D, \lambda_0, p, n, c) &= V(t, D, \lambda_0, p, n) \exp(-bc\lambda_0 t) \\
 b &= \frac{2\pi\mu_0 g_A g_B \mu_B^2}{9\sqrt{3}h}
 \end{aligned}
 \quad (8)$$

where  $b$  is a constant for the intermolecular PELDOR background in three-dimensional homogeneous distributions [16] and  $c$  is the spin-label concentration in  $m^{-3}$ . Under constant experimental conditions,  $\lambda_0$  can be assumed constant and measured using a standard biradical [29,31].

The PELDOR time traces in micelles can be simulated according to Eq. (8). *Vice versa* the micelle parameters can be verified by a fit of  $D$ ,  $p$ ,  $n$ , and  $c$  to the experimental time traces.

### 3. Materials and methods

#### 3.1. Materials

$n$ -Dodecyl  $\beta$ -D-maltoside (DDM;  $\geq 99.0\%$ ), and sodium phosphate (20 mM solution; pH 7.0) were obtained from Fluka. 5- and 16-doxyl-stearic acid (5- and 16-SASL) spin-labels, octaethylene glycol monododecyl ether ( $C_{12}E_8$ ;  $\geq 98\%$ ), and sodium dodecyl sulfate (SDS;  $\geq 99.0\%$ ) were purchased from Sigma–Aldrich (Germany). Polyethyleneglycol-mono-[ $p$ -(1,1,3,3-tetra methylbutyl)-phenyl]-ether (Triton<sup>®</sup> X-100) was obtained from AppliChem GmbH, Germany.

#### 3.2. Sample preparation

20 mM solutions of the detergents (above their critical micelle concentration (CMC) at 25 °C) were prepared in phosphate buffer, except for the SDS sample which was prepared in double-distilled water. Stock solutions of 5- and 16-SASL (2 and 27 mM, respec-

tively) were prepared in chloroform and the concentrations have been calibrated against TEMPO by use of an Elexsys E500 9 GHz EPR spectrometer (Bruker). In order to prepare the samples of the spin-labeled stearic acids in different micelles with the desired spin-label to detergent molar ratio, the required amounts of the spin-labels in chloroform were transferred to test tubes, the solvent was evaporated with an argon gas stream, and residual traces were removed by drying under vacuum for at least 4 h before the vacuum was released by nitrogen. The prepared micelle solutions were added to the preformed films of the spin-labels. The samples were shaken by vortex mixing at room temperature and kept overnight in a 4 °C fridge to equilibrate them. All the samples were mixed with 20% (v/v) ethylene glycol and transferred to standard 4 mm diameter quartz EPR tubes (Wilmad). The samples were shock-frozen in a mixture of methylcyclohexane/isopentane (1:4) that was immersed in liquid nitrogen.

#### 3.3. EPR experiments

Pulsed EPR data were measured on an Elexsys E580 EPR spectrometer (Bruker) equipped with a Bruker PELDOR unit (E580-400U), a continuous-flow helium cryostat (CF935) and temperature control system (ITC 502), both from Oxford Instruments, at frequencies of  $\sim 9.6$  GHz (X-band) using a standard flex line probe head housing a dielectric ring resonator (MD5 W1, Bruker). Microwave pulses were amplified by a 1 kW TWT amplifier (ASE 117x). Temperature was kept at 50 K. The shot repetition time was 2–3 ms.

For PELDOR experiments the dead-time free four-pulse sequence was used [6,32]. The  $\pi/2$ -pulse was phase-cycled (+/–) to eliminate receiver offsets [26]. Typical pulse lengths were 32 ns ( $\pi/2$  and  $\pi$ ) for the probe pulses and 14 ns ( $\pi$ ) for the pump pulse. The delay between the first and second probe pulses was varied between 136 and 192 ns in 8 ns steps to reduce the contributions from proton hyperfine modulations [33]. The pulse separation between the second and third probe pulses was between 2 and 3  $\mu$ s, depending on the transversal relaxation time ( $T_m$ ) of the samples. The frequency of the pump pulse was set to center of the over-coupled resonator ( $Q \sim 50$ ) and the magnetic field was adjusted, such that the excitation coincides with the central peak of the nitroxide powder spectrum to obtain maximum pumping efficiency. The probe frequency was chosen 70 MHz higher.

#### 3.4. Data processing

To obtain distance distributions, the PELDOR data were processed using the DeerAnalysis2008 software package [26]. The PELDOR time traces were corrected for background decay using a homogeneous three-dimensional spin distribution. Tikhonov regularizations have been performed with a regularization parameter ( $\alpha$ ) of 1000.

To obtain the micelle parameters the root mean square deviation between experimental data and calculated  $V_{total}$  (Eq. (8)) has been minimized for both models individually using the Matlab<sup>®</sup> function `fminsearch`.  $D$ ,  $p$ ,  $n$  and  $c$  have been optimized simultaneously. The integrations in Eq. (6) have been performed numerically in steps of 0.01 nm and  $10^{-3}$  respectively. Distributions of micelle sizes and aggregation numbers have not been considered. Multiple labeled micelles ( $k$ ) with a statistical weight smaller than  $10^{-4}$  have been neglected. To explore the effects of the strong interdependence of  $p$  and  $n$ , which both mainly scale the modulation depth, a second optimization has been performed. Here,  $p$  has been set to the nominal labeling degree while  $D$ ,  $n$  and  $c$  being simultaneously optimized.

#### 4. Results and discussion

The experimental PELDOR time traces for two different spin-labeled fatty acids (5-SASL and 16-SASL) incorporated into several micelles (DDM, SDS,  $C_{12}E_8$  and Triton X-100) are shown in Fig. 2. All of them exhibit a fast initial decay and a slow decay component which persist for the length of the observation window. None of the traces can be fitted by a stretched exponential decay function. To remove the homogeneous inter-micellar background the time traces have been divided by an exponential decay function fitting the slow component. The modulation depth for most of the samples are rather similar (27–32%); only the sample of 3 mole% 16-SASL in DDM shows a somewhat larger value of 38%. For 16-SASL the mean distances, obtained from the time traces by Tikhonov regularization are all between 2 and 2.5 nm (Fig. 3). Given the broad distance distribution width ( $\sigma(r) \sim 0.6\text{--}1.3$  nm) they are rather similar. In the case of 5-SASL in DDM the mean distance is significantly shifted to almost 3 nm.

These distinct distances are not caused by specific interactions between the spin-labeled fatty acids but reflect the distance restrictions imposed by the finite micelle dimensions. It is important to note that we cannot rule out the presence of specific interactions between spin-labels. However, utilizing the same spin-labels in phospholipid vesicle membranes homogeneous distributions have been observed. Thus, there is no indication of specific interactions [15]. Furthermore, if the spin-labels form specific

structures with short spin–spin distances, their dipolar coupling will be too large to be excited by the microwave pulses. Thus, we can neglect their contribution to the PELDOR signal in good approximation. Simulations based on the *surface* and *bulk* distribution model together with their deviation from the experimental PELDOR time traces are shown in Fig. 2. The parameters ( $n$ ,  $D$ ,  $c$  and  $p$ ) of both models, *surface* and *bulk*, have been optimized by minimizing the root mean square deviation between the experimental data and the simulation based on Eq. (8). Both models show a very good agreement with the experimental PELDOR time traces. The *surface* model exhibits a slightly larger divergence. This model predicts a large contribution from spin pairs at the maximum distance (Fig. 3c) leading to a shallow but distinct dipolar modulation in the simulations. This oscillation is not visible in the experimental data; however, already a moderate distribution in micelle diameters will easily diminish this oscillation. The optimal fitting parameters for  $n$ ,  $D$ ,  $c$  and  $p$  are summarized in Table 1. The initial fast decay of the time traces can be attributed to the dipolar interaction of spin-labels within one micelle, whereas the slower decay results from the dipolar interactions between spin-labels in different micelles. The different influence of the parameters  $n$ ,  $D$ ,  $c$  and  $p$  on the PELDOR time traces is noteworthy. The micelle diameter  $D$  mostly influences the fast initial decay of the PELDOR time traces, whereas the spin-label concentration  $c$  determines the slope of the slowly decaying part. In contrast, both  $n$  and  $p$  contribute mainly to the modulation depth and have only minor effects on the fast

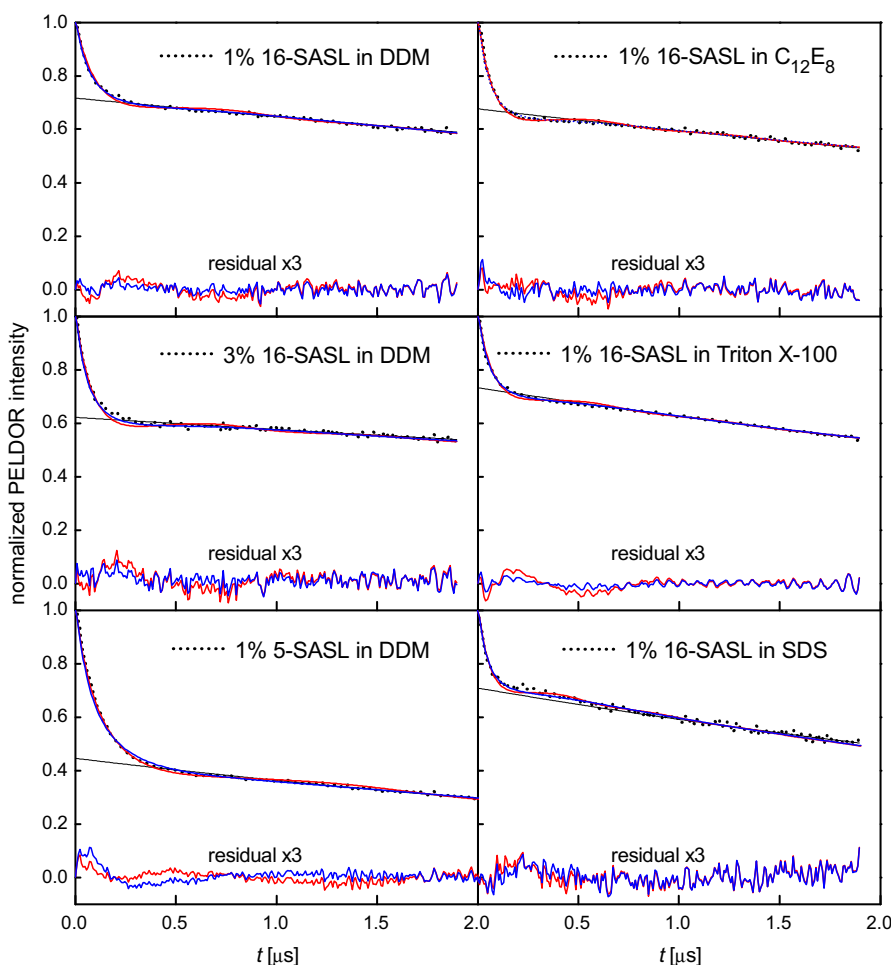


**Fig. 2.** The model fits in different detergent micelles. Experimental data is given in dotted black, the PELDOR background functions in solid black, surface model in red and the bulk model in blue. Below each trace the residual of experimental data minus simulation multiplied by three is displayed. (For interpretation of the references to colour in this figure legend, the reader is referred to the web version of this article.)

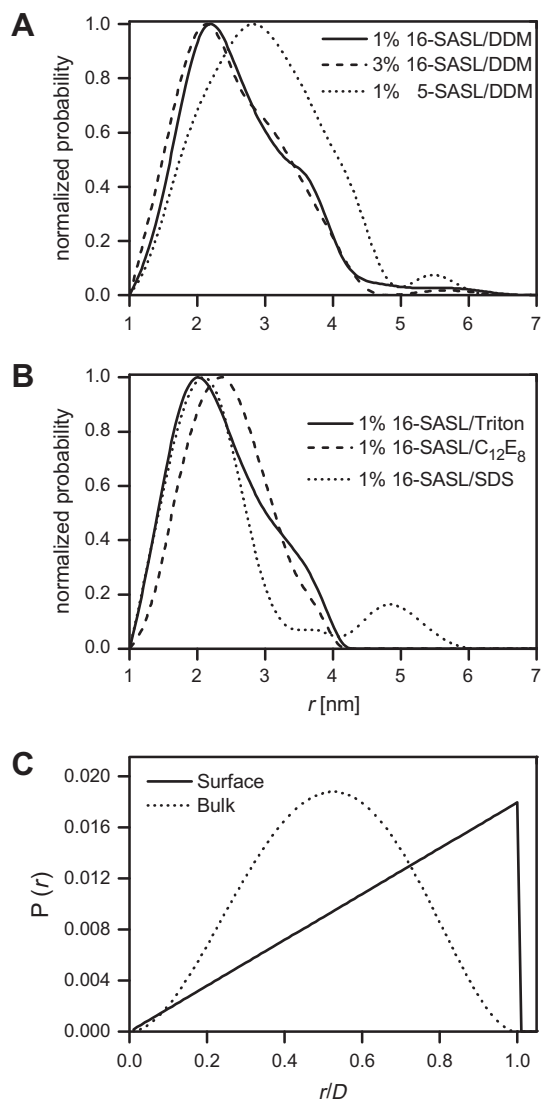


**Fig. 3.** Distance distributions. (A and B) Obtained distance distributions from Tikhonov regularization for different detergent micelles; (C) Distance probability densities for the two different distribution models in micelles.

initial decay of the PELDOR time traces. In principle,  $p$  governs the amount of multi-spin effects [30] and, thus, also contributes to the dipolar evolution caused by spin-labels within one micelle. In cases of broad distance distributions and moderate labeling degrees these effects are usually not resolved experimentally [29]. As a consequence, these two parameters are strongly interdependent. To separate them, we also fitted all time traces by fixing  $p$  to the nominal labeling degree. For 16-SASL, simulations with both models reproduce the literature values for  $D$  nicely [21,34]. It is important to note that micelle diameters are usually derived from the radius of gyration including a solvent shell. However, in the present study the nitroxide moiety is expected to be located between the micelle's hydrophobic core and the polar-apolar interface, well inside of this solvent shell. 5-SASL results in larger micelle diameters. This might be caused by a distortion of the micelle by the labeling close to the head-group. Otherwise, it might indicate that neither model fully reflects the real distribution in the micelle. The polar head-group of the fatty acid is assumed to be restricted to the polar-apolar interface close to the micelle surface. In this case, the nitroxide moiety of 5-SASL can occupy a spherical shell with a bigger mean radius as compared to 16-SASL. A shorter linker between

head-group and nitroxide moiety restricts the nitroxide to the periphery of the micelle. Thus, in the approximation that the variations of radii of this spherical shell arise from the length of this linker, the variation of radii will be much smaller for 5-SASL as it is much more closely linked to the head-group.

Considerably more uncertainties are related to the obtained fit values for  $n$  and  $p$  as long as none of them can be independently determined to high precision. Already a small amount of free spin-label in the solution would effect  $p$  [25]. Furthermore, the literature values for  $n$  show a significant spread. Therefore the values of these parameters extracted from both models should be taken only as rough estimates. Nevertheless, the analysis based on both of our models yields micelle properties which are in reasonable agreement with values obtained by luminescence quenching [35], sedimentation techniques [21], small angle X-ray scattering [34] and positron lifetime spectroscopy [36].

Our results clearly show, that in micellar systems PELDOR time traces with a distinct initial decay are not a decisive indication of a specific aggregate but a result of the finite size of the micelle. In extreme cases, even the observation of a dipolar modulation, as present in the simulations using the *surface* model, might be caused by size restriction effects rather than specific interactions [37]. This might be important for the study of homo-oligomeric systems, such as lipophilic peptides or membrane proteins in detergent micelles, were such PELDOR signals could be easily misinterpreted to represent structural information on the macromolecular complex itself. As we have shown here, a signal deviating from a stretched exponential alone does not allow discriminating between specific and unspecific clustering. The assumption, that the observed dipolar interaction represents a specific interaction and not statistical segregation into the micelles will have to be confirmed by further evidence. Wherever possible a system in which the desired specific interaction has been switched off by design (the 'singly-labeled' reference) should be measured. Through this control the unspecific PELDOR background function could be identified. The observation of significant differences between the sample and its control will allow relevant structural conclusions. In general, it seems unlikely to solve the problem of the background theoretically without utilizing a 'singly-labeled' reference sample. Obviously, the solution to this problem is not trivial. In principle, the singly-labeled reference can be obtained by cross-linking the oligomer under study and expressing it as a single polypeptide chain that only contains a single cysteine residue. This sample could act as singly-labeled reference. However, such a construct might not always be feasible. On the other hand, lowering the local concentration of spin-labeled molecules by decreasing their overall concentration can be used to test if size restriction effects blur the analysis of specific interactions by PELDOR. If the oligomer under study exhibits strong binding and the monomers do not exchange, the multiply-labeled oligomer could be diluted with unlabeled oligomer to achieve a similar effect.

## 5. Conclusion

We have investigated statistically partitioned spin-labeled molecules into detergent micelles. The resulting PELDOR time-domain signals cannot be described with a stretched exponential decay function, as would be expected in homogeneous solutions or in lipid vesicle membranes, but could be quantitatively modeled based on the size of the micelles, their aggregation number, spin-label concentration and the spin-labeling degree. The labeling degree  $p$  and aggregation number  $n$  showed a strong interdependence, thus, they could not be determined independently to high precision. On the other hand, the local concentration  $c$  and micelle diameter  $D$  could be determined rather accurately from the PELDOR data. A

**Table 1**  
Relevant micelle and sample parameters.

Sample	Triton X-100 1% 16-SASL	SDS 1% 16-SASL	C12E8 1% 16-SASL	DDM 1% 5-SASL	DDM 3% 16-SASL	DDM 1% 16-SASL
<i>n</i>	75 <sup>a</sup> , 140 <sup>a</sup> , 96-165 <sup>a</sup>	62 <sup>b</sup>	89 <sup>a</sup> , 98 <sup>a</sup> , 120 <sup>a</sup>	110 <sup>a</sup> , 126 <sup>a</sup> , 111-140 <sup>a</sup> , 78-149 <sup>c</sup> , 140 <sup>c</sup> , 135-145 <sup>c</sup>	110 <sup>a</sup> , 126 <sup>a</sup> , 111-140 <sup>a</sup> , 78-149 <sup>c</sup> , 140 <sup>c</sup> , 135-145 <sup>c</sup>	110 <sup>a</sup> , 126 <sup>a</sup> , 111-140 <sup>a</sup> , 78-149 <sup>c</sup> , 140 <sup>c</sup> , 135-145 <sup>c</sup>
<i>D</i> [nm]	6.84 <sup>a</sup> , 7.50 <sup>a</sup>	3.38-3.7 <sup>d</sup> , 3.1 (core) <sup>a</sup>	6.44 <sup>a</sup> , 8.04 <sup>a</sup> , 3.1 (core) <sup>a</sup>	5.98 <sup>a</sup> , 6.24 <sup>a</sup> , 2.82-5.8 <sup>c</sup> , 3.1 (core) <sup>a</sup>	5.98 <sup>a</sup> , 6.24 <sup>a</sup> , 2.82-5.8 <sup>c</sup> , 3.1 (core) <sup>a</sup>	5.98 <sup>a</sup> , 6.24 <sup>a</sup> , 2.82-5.8 <sup>c</sup> , 3.1 (core) <sup>a</sup>
<i>c</i> <sub>surface</sub> [μM]	316 <sup>e</sup> , 316 <sup>f</sup>	430 <sup>e</sup> , 430 <sup>f</sup>	252 <sup>e</sup> , 255 <sup>f</sup>	436 <sup>e</sup> , 435 <sup>f</sup>	167 <sup>e</sup> , 208 <sup>f</sup>	229 <sup>e</sup> , 228 <sup>f</sup>
<i>n</i> <sub>surf</sub>	110 <sup>e</sup> , 139 <sup>f</sup>	121 <sup>e</sup> , 144 <sup>f</sup>	143 <sup>e</sup> , 170 <sup>f</sup>	217 <sup>e</sup> , 272 <sup>f</sup>	244 <sup>e</sup> , 67 <sup>f</sup>	116 <sup>e</sup> , 136 <sup>f</sup>
<i>p</i> <sub>surf</sub>	1.27% <sup>e</sup> , 1% <sup>f</sup>	1.19% <sup>e</sup> , 1% <sup>f</sup>	1.19% <sup>e</sup> , 1% <sup>f</sup>	1.26% <sup>e</sup> , 1% <sup>f</sup>	0.79% <sup>e</sup> , 3% <sup>f</sup>	1.17% <sup>e</sup> , 1% <sup>f</sup>
<i>D</i> <sub>surf</sub> [nm]	3.20 <sup>e</sup> , 3.23 <sup>f</sup>	2.91 <sup>e</sup> , 2.91 <sup>f</sup>	3.26 <sup>e</sup> , 3.26 <sup>f</sup>	4.29 <sup>e</sup> , 4.30 <sup>f</sup>	3.44 <sup>e</sup> , 2.91 <sup>f</sup>	3.56 <sup>e</sup> , 3.57 <sup>f</sup>
<i>c</i> <sub>bulk</sub> [μM]	310 <sup>e</sup> , 309 <sup>f</sup>	423 <sup>e</sup> , 423 <sup>f</sup>	244 <sup>e</sup> , 243 <sup>f</sup>	416 <sup>e</sup> , 417 <sup>f</sup>	159 <sup>e</sup> , 158 <sup>f</sup>	221 <sup>e</sup> , 221 <sup>f</sup>
<i>n</i> <sub>bulk</sub>	110 <sup>e</sup> , 142 <sup>f</sup>	123 <sup>e</sup> , 145 <sup>f</sup>	132 <sup>e</sup> , 172 <sup>f</sup>	161 <sup>e</sup> , 273 <sup>f</sup>	48 <sup>e</sup> , 65 <sup>f</sup>	143 <sup>e</sup> , 138 <sup>f</sup>
<i>p</i> <sub>bulk</sub>	1.29% <sup>e</sup> , 1% <sup>f</sup>	1.18% <sup>e</sup> , 1% <sup>f</sup>	1.30% <sup>e</sup> , 1% <sup>f</sup>	1.70% <sup>e</sup> , 1% <sup>f</sup>	4.07% <sup>e</sup> , 3% <sup>f</sup>	0.96% <sup>e</sup> , 1% <sup>f</sup>
<i>D</i> <sub>bulk</sub> [nm]	4.19 <sup>e</sup> , 4.18 <sup>f</sup>	3.88 <sup>e</sup> , 3.89 <sup>f</sup>	4.28 <sup>e</sup> , 4.27 <sup>f</sup>	5.75 <sup>e</sup> , 5.75 <sup>f</sup>	4.50 <sup>e</sup> , 4.50 <sup>f</sup>	4.63 <sup>e</sup> , 4.63 <sup>f</sup>

<sup>a</sup> From [21].

<sup>b</sup> From [35].

<sup>c</sup> From [34].

<sup>d</sup> From [36].

<sup>e</sup> Diameter *D*, labeling probability *p*, aggregation number *n* and concentration *c* have been optimized simultaneously.

<sup>f</sup> *D*, *n* and *c* have been optimized simultaneously, *p* has been set to the nominal labeling degree.

clear distinction between situations where the spin-labels are distributed homogeneously within the micelle or within a narrow spherical shell at the polar-apolar interface is not possible, as can be seen from our simulations with both models. Both models give satisfactory agreement with the experimental data, with slightly different best fit values for the micelle diameter *D*. In conclusion, we show very clear evidence that a PELDOR time-domain signal in detergent micelles differing from a stretched exponential is not sufficient to prove a specific interaction. This might obscure structural investigations on incorporated macromolecules or complexes. In such systems further evidence will have to be presented to ensure that the measured distance distribution is not related to such micellar size effects.

## Acknowledgments

We thank Deniz Sezer (Sabanci University) and Andriy Marko for many inspiring discussions and Ivan Krstic, Vasyl Denysenko and Sevdalina Lyubenova for carefully reading the manuscript. We acknowledge the Collaborative Research Center SFB 807 “Transport and Communication across Membranes” of the German Research Society (DFG), the Center of Biomolecular Magnetic Resonance (BMRZ) and the DFG-funded Center of Excellence: “Macromolecular Complexes” for financial support. B.E.B. is currently supported by a Feodor-Lynen fellowship by the Alexander von Humboldt Foundation financed by the German Federal Ministry of Education and Research and a Marie Curie Intra European Fellowship within the 7th European Community Framework Programme.

## References

- [1] A.D. Milov, K.M. Salikov, M.D. Shirov, Application of ELDOR in electron-spin echo for paramagnetic center space distribution in solids, *Fiz. Tverd. Tela* 23 (1981) 975.
- [2] A.D. Milov, A.B. Ponomarev, Y.D. Tsvetkov, Electron–electron double resonance in electron spin echo: model biradical systems and sensitized photolysis of decalin, *Chem. Phys. Lett.* 110 (1984) 67–72.
- [3] G. Jeschke, Y. Polyhach, Distance measurements on spin-labelled biomacromolecules by pulsed electron paramagnetic resonance, *Phys. Chem. Chem. Phys.* 9 (2007) 1895–1910.
- [4] O. Schiemann, T.F. Prisner, Long-range distance determinations in biomacromolecules by EPR spectroscopy, *Quart. Rev. Biophys.* 40 (2007) 1–53.
- [5] V. Pfannebecker, H. Klos, M. Hubrich, T. Volkmer, A. Heuer, U. Wiesner, H.W. Spiess, Determination of end-to-end distances in oligomers by pulsed EPR, *J. Phys. Chem.* 100 (1996) 13428–13432.
- [6] M. Pannier, S. Veit, A. Godt, G. Jeschke, H.W. Spiess, Dead-time free measurement of dipole–dipole interactions between spins, *J. Magn. Reson.* 142 (2000) 331–340.
- [7] A. Weber, O. Schiemann, B. Bode, T.F. Prisner, PELDOR at S- and X-Band frequencies and the separation of exchange coupling from dipolar coupling, *J. Magn. Reson.* 157 (2002) 277–285.
- [8] Z. Zhou, S.C. DeSensi, R.A. Stein, S. Brandon, M. Dixit, E.J. McArdle, E.M. Warren, H.K. Kroh, L. Song, C.E. Cobb, E.J. Hustedt, A.E. Beth, Solution structure of the cytoplasmic domain of erythrocyte membrane band 3 determined by site-directed spin labeling, *Biochemistry* 44 (2005) 15115–15128.
- [9] J.E. Banham, C.R. Timmel, R.J.M. Abbott, S.M. Lea, G. Jeschke, The characterization of weak protein–protein interactions: evidence from DEER for the trimerization of a von Willebrand Factor A domain in solution, *Angew. Chem. Int. Ed.* 45 (2006) 1058–1061.
- [10] O. Schiemann, A. Weber, T.E. Edwards, T.F. Prisner, S.T. Sigurdsson, Nanometer distance measurements on RNA using PELDOR, *J. Am. Chem. Soc.* 125 (2003) 3434–3435.
- [11] O. Schiemann, N. Piton, Y. Mu, G. Stock, J.W. Engels, T.F. Prisner, A PELDOR-based nanometer distance ruler for oligonucleotides, *J. Am. Chem. Soc.* 126 (2004) 5722–5729.
- [12] G. Jeschke, Determination of the nanostructure of polymer materials by electron paramagnetic resonance spectroscopy, *Macromol. Rapid Commun.* 23 (2002) 227–246.
- [13] A.D. Milov, D.A. Erilov, E.S. Salmikov, Y.D. Tsvetkov, F. Formaggio, C. Toniolo, J. Raap, Structure and spatial distribution of the spin-labelled lipopeptide trichogin GA IV in a phospholipid membrane studied by pulsed electron–electron double resonance (PELDOR), *Phys. Chem. Chem. Phys.* 7 (2005) 1794–1799.
- [14] A.D. Milov, R.I. Samoilova, Y.D. Tsvetkov, F. Formaggio, C. Toniolo, J. Raap, Membrane–peptide interaction studied by PELDOR and CW ESR: Peptide conformations and cholesterol effect on the spatial peptide distribution in the membrane, *Appl. Magn. Reson.* 29 (2005) 703–716.
- [15] R. Dastvan, B.E. Bode, M.P.R. Karuppiah, A. Marko, S. Lyubenova, H. Schwalbe, T.F. Prisner, Optimization of transversal relaxation of nitroxides for pulsed electron–electron double resonance spectroscopy in phospholipid membranes, *J. Phys. Chem. B* 114 (2010) 13507–13516.
- [16] A.D. Milov, A.G. Maryasov, Y.D. Tsvetkov, Pulsed electron double resonance (PELDOR) and its applications in free-radicals research, *Appl. Magn. Reson.* 15 (1998) 107–143.
- [17] S. Ruthstein, A. Potapov, A.M. Raitsimring, D. Goldfarb, Double electron resonance as a method for characterization of micelles, *J. Phys. Chem. B* 109 (2005) 22843–22851.
- [18] S. Ruthstein, D. Goldfarb, Evolution of solution structures during the formation of the cubic mesoporous material, KIT-6, determined by double electron–electron resonance, *J. Phys. Chem. C* 112 (2008) 7102–7109.
- [19] Q. Mao, S. Schleidt, H. Zimmermann, G. Jeschke, A pulsed EPR study of surfactant layer structure in composites of a synthetic layered silicate with polystyrene and polycaprolactone, *Phys. Chem. Chem. Phys.* 10 (2008) 1156–1167.
- [20] P. Ionita, A. Volkov, G. Jeschke, V. Chechik, Lateral diffusion of thiol ligands on the surface of Au nanoparticles: an electron paramagnetic resonance study, *Anal. Chem.* 80 (2008) 95–106.

- [21] J.V. Moller, M. Lemaire, Detergent binding as a measure of hydrophobic surface-area of integral membrane-proteins, *J. Biol. Chem.* 268 (1993) 18659–18672.
- [22] P. Baglioni, L. Dei, E. Rivara-Minten, L. Kevan, Mixed micelles of SDS/C<sub>12</sub> E<sub>6</sub> and DTAC/C<sub>12</sub> E<sub>6</sub> surfactants, *J. Am. Chem. Soc.* 115 (1993) 4286–4290.
- [23] R.D. Lord, The distribution of distance in a hypersphere, *Ann. Math. Stat.* 25 (1954) 794–798.
- [24] M. Parry, E. Fischbach, Probability distribution of distance in a uniform ellipsoid: Theory and applications to physics, *J. Math. Phys.* 41 (2000) 2417–2433.
- [25] L.R. Brown, C. Bosch, K. Wuthrich, Location and orientation relative to the micelle surface for Glucagon in mixed micelles with dodecylphosphocholine - EPR and NMR studies, *Biochim. Biophys. Acta* 642 (1981) 296–312.
- [26] G. Jeschke, V. Chechik, P. Ionita, A. Godt, H. Zimmermann, J. Banham, C.R. Timmel, D. Hilger, H. Jung, DeerAnalysis2006 a comprehensive software package for analyzing pulsed ELDOR data, *Appl. Magn. Reson.* 30 (2006) 473–498.
- [27] B.E. Bode, J. Plackmeyer, T.F. Prisner, O. Schiemann, PELDOR measurements on a nitroxide-labeled Cu(II) porphyrin: orientation selection, spin-density distribution, and conformational flexibility, *J. Phys. Chem. A* 112 (2008) 5064–5073.
- [28] D. Margraf, B.E. Bode, A. Marko, O. Schiemann, T.F. Prisner, Conformational flexibility of nitroxide biradicals determined by X-band PELDOR experiments, *Mol. Phys.* 105 (2007) 2153–2160.
- [29] B.E. Bode, D. Margraf, J. Plackmeyer, G. Dürner, T.F. Prisner, O. Schiemann, Counting the monomers in nanometer-sized oligomers by pulsed electron-electron double resonance, *J. Am. Chem. Soc.* 129 (2007) 6736–6745.
- [30] G. Jeschke, M. Sajid, M. Schulte, A. Godt, Three-spin correlations in double electron-electron resonance, *Phys. Chem. Chem. Phys.* 11 (2009) 6580–6591.
- [31] D. Hilger, H. Jung, E. Padan, C. Wegener, K.-P. Vogel, H.-J. Steinhoff, G. Jeschke, Assessing oligomerization of membrane proteins by four-pulse DEER: pH-Dependent Dimerization of NhaA Na<sup>+</sup>/H<sup>+</sup> Antiporter of *E. coli*, *Biophys. J.* 89 (2005) 1328–1338.
- [32] R.E. Martin, M. Pannier, F. Diederich, V. Gramlich, M. Hubrich, H.W. Spiess, Determination of end-to-end distances in a series of TEMPO Diradicals of up to 2.8 nm length with a new four-pulse double electron resonance experiment, *Angew. Chem. Int. Ed.* 37 (1998) 2833–2837.
- [33] G. Jeschke, G. Panek, A. Godt, A. Bender, H. Paulsen, Data analysis for pulse ELDOR measurements of broad distance distributions, *Appl. Magn. Reson.* 26 (2004) 223–244.
- [34] J. Lipfert, L. Columbus, V.B. Chu, S.A. Lesley, S. Doniach, Size and shape of detergent micelles determined by small-angle X-ray scattering, *J. Phys. Chem. B* 111 (2007) 12427–12438.
- [35] N.J. Turro, A. Yekta, Luminescent probes for detergent solutions. A simple procedure for determination of the mean aggregation number of micelles, *J. Am. Chem. Soc.* 100 (1978) 5951–5952.
- [36] G. Duplatre, M.F. Ferreira Marques, M. daGracaMiguel, Size of sodium dodecyl sulfate micelles in aqueous solutions as studied by positron annihilation lifetime spectroscopy, *J. Phys. Chem.* 100 (1996) 16608–16612.
- [37] O. Schiemann, Mapping Global Folds of Oligonucleotides by Pulsed Electron-Electron Double Resonance, *Methods in Enzymology, Biophysical, Chemical, and Functional Probes of RNA Structure, Interactions and Folding*, Pt B, vol. 469, Elsevier Academic Press Inc., San Diego, 2009. pp. 329–351.